OLYMPUS Status Report

OLYMPUS Collaboration

1 Introduction

This is intended to be a brief report on developments regarding the OLYMPUS experiment since the last PRC meeting.

At the last PRC meeting we reported on several topics:

- the analysis of the detector position survey ($< 100\ \mu$m),
- fitting the magnetic field measurements (< 19 G),
- the beam energy calibration (0.01%),
- studies to understand and optimize the Møller/Bhabha calorimeter and the 12° GEM and MWPC telescopes,
- the calibration of the time of flight detectors,
- the first tracking results using the elastic arm algorithm with a preliminary yield distribution, and
- the status of our Monte Carlo generator including radiative corrections.

During the closed session we outlined our immediate plans:

- additional manpower to work on the luminosity detectors,
- separate fit to the magnetic field in the region of the symmetric Møller/Bhabha event trajectories,
- beam position monitor calibration,
- improve detector calibrations using tracking, and

- Monte Carlo simulation with radiative corrections.

The recommendations from the PRC added:

- completing the digitization of all detectors in the Monte Carlo,
- increasing manpower and expertise on software and analysis, and
- developing an alternative, traditional approach to tracking reconstruction,

The PRC report also requested that this report address the luminosity determination and characterize the tracking performance.

In the following we will try to address all of the above. The work is not finished and there have been set-backs but steady progress is being made. For brevity point-form will be used as much as possible. Detailed descriptions or explainations, if needed, are perhaps more easily communicated via phone or video conference if necessary.

2 Manpower

The principal people working on the OLYMPUS analysis are outlined in the following included the area(s) in which they are active. This is not complete and certainly several names are missing for simplicity. Results for several topics are given in following sections.

- D. Khaneft (Mainz) is taking a more active role on the SYMB. He came to MIT from mid-November to mid-December to gain experience with the analysis framework and is now working on the digitization of the SYMB. Dmitry joins R. Perez Benito (Mainz) who is also working on the SYMB (see below).
- C. O'Connor (MIT) is now also working on the SYMB analysis (see below).
- U. Schneekloth (DESY) has completed the BPM survey, calibration, analysis (see below) needed for the SYMB analysis.
- B. Henderson (MIT) is now working on the analysis of 12° detector telescopes (see below). Unfortunately Ö. Ates (Hampton) will be leaving shortly. D. Veretennikov (PNPI) continues working on the MWPC.
- L.D. Ice (ASU), R. Russell (MIT), and N. Akopov (AANL) continue caring for the TOF calibration, simulation, and analysis now using the reconstructed tracking information (see below).

- R. Russell (MIT) and A. Schmidt (MIT) have mostly finished the Monte Carlo generator incorporating radiative corrections (see below).
- J. Bernauer (MIT) continues work on track reconstruction extending the tracks to the TOF detectors (see below). He also serves as software coordinator and directs most of the analysis efforts.
- D. Hasell (MIT) is pursuing an alternative approach to track reconstruction (see below) when he is not writing reports.
- M. Kohl (Hampton) continues as luminosity and physics coordinator. Unfortunately J. Diefenbach (now at Mainz) who contributed so much has less time to help with OLYMPUS.
- N. D'Ascenzo (DESY) and N. Akopov (AANL) are working on analyzing the reconstructed track data (see below).

3 Luminosity

The OLYMPUS luminosity monitors include the symmetric Møller/Bhabha detector and the 12° telescopes of GEM and MWPC detectors.

3.1 Symmetric Moller / Bhabha Calorimeter

The symmetric Møller/Bhabha detector, SYMB, should provide our best measure of the luminosity. There are two parts to this: first, getting a stable, reliable measure of the number of symmetric scattering events, and, second, accurately simulating the processes with the Monte Carlo.

- R. Perez Benito has been working on a dynamic non-linearity algorithm to smooth the histograms produced by the SYMB electronics so the coincidence peak can be more accurately found, fit, and integrated. This is illustrated in Fig. 1. With this the ratio found between electron and positron runs is 1.640 ± 0.006.
- R. Perez Benito (Mainz) has also measured that the SYMB pedestals are stable over time and do not contribute any noticeable affect.

- as mentioned D. Khaneft (Mainz) is working on simulating the SYMB in the Monte Carlo.
- C. O'Connor (MIT) has been investigating the SYMB also with Monte Carlo. One of the questions was the "legs" to the left and right of the coincidence peak observed in the data (see Fig. 2. These are qualitatively reproduced in the Monte Carlo and found to arise from events near the edge of the collimator on one side with the corresponding, symmetric scattered particle striking the edge of the collimator on the other side. This other particle showers or multiple scatters resulting in energy loss producing the "legs".
- The previous plots showed the SYMB coincidence histogram with a logarithmic scale. Plotted with a linear scale, Fig. 3, the coincidence peak is clearly separated from an almost flat background. Applying a square graphical cut centered at (1.95, 1.95) and comparing the integral as a function of the box size shows that the changes to the integral are less significant as the box size grows and plateaus for a box size around 80 × 80.
- A separate fit to the measured magnetic field data in the volume important to the SYMB was made by B. Henderson (MIT) and A. Schmidt (MIT) to yield the fits needed for tracking SYMB events in the Monte Carlo. The resulting small field (< ±30 G) are shown in Fig. 4.

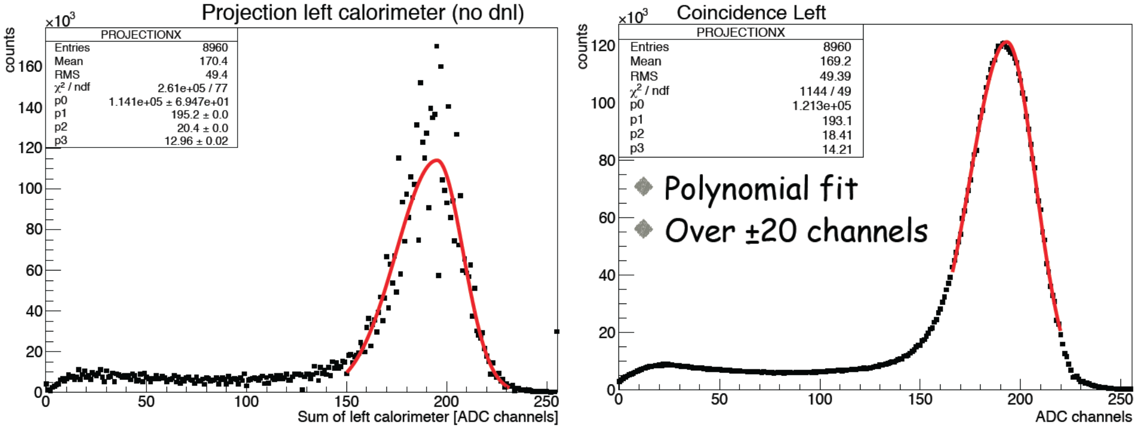

(a) Without DNL

(b) After DNL

Figure 1: Effect of dynamic nonlinearity correction to SYMB histograms.

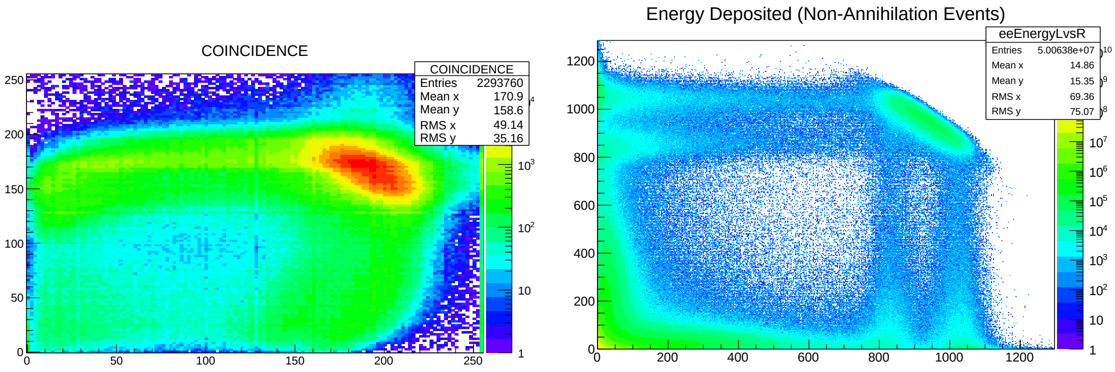

(a) Data

(b) Monte Carlo

Figure 2: Symmetric Møller/Bhabha coincidences plots with a logarithmic scale.

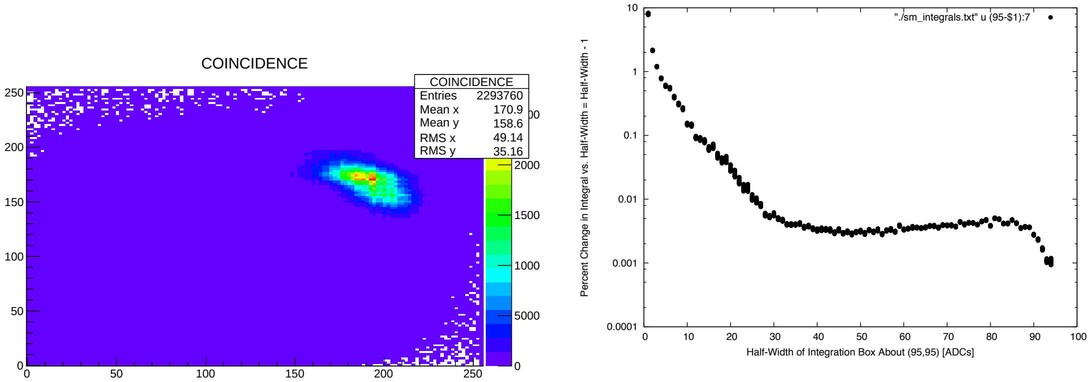

(a) Data

(b) Change in integral

Figure 3: Symmetric Møller/Bhabha coincidence plot with a linear scale.

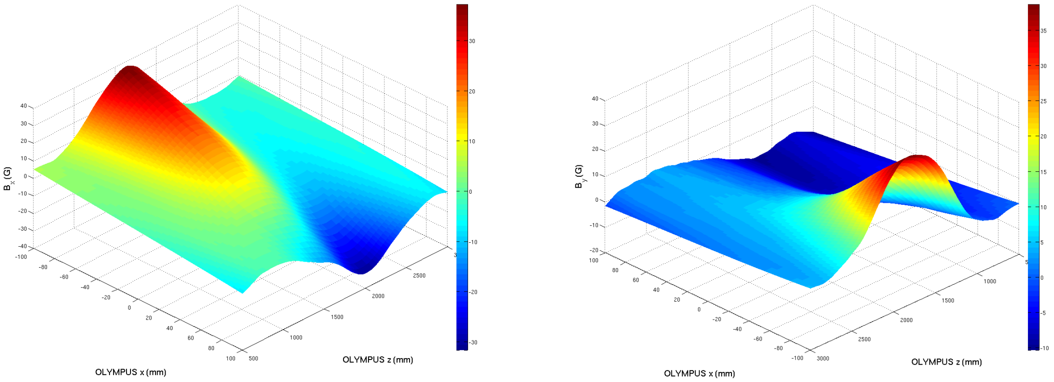

(a) B_x (b) B_y

Figure 4: Optimized magnetic field values in the volume relevant for the symmetric Møller/Bhabha detectors.

3.2 Beam Position Monitors

- U. Schneekloth (DESY) organized and analyzed the calibration of the beam position monitors, BPMs.
- Knowledge of the beam position during data taking is crucial in analyzing the SYMB luminosity because the small angle, 1.29°, for symmetric scattering is very sensitive to the beam position and slope.
- The BPMs upstream and downstream of the target were readout by two systems: Neumann and Libera. Only the first was available for the Spring 2012 running period. Only the Libera system was available in 2013 when the offline calibration was performed.
- The calibration was performed offline using a test stand with a current flowing in a wire positioned inside the BPMs. The wire position was surveyed and adjusted by micrometer screws.
- To compare the Neumann data theTina database of DORIS machine parameters was used.
- The results of the calibration and comparison are summarized in Fig. 5 and show the calibration is knower at the few percent level.

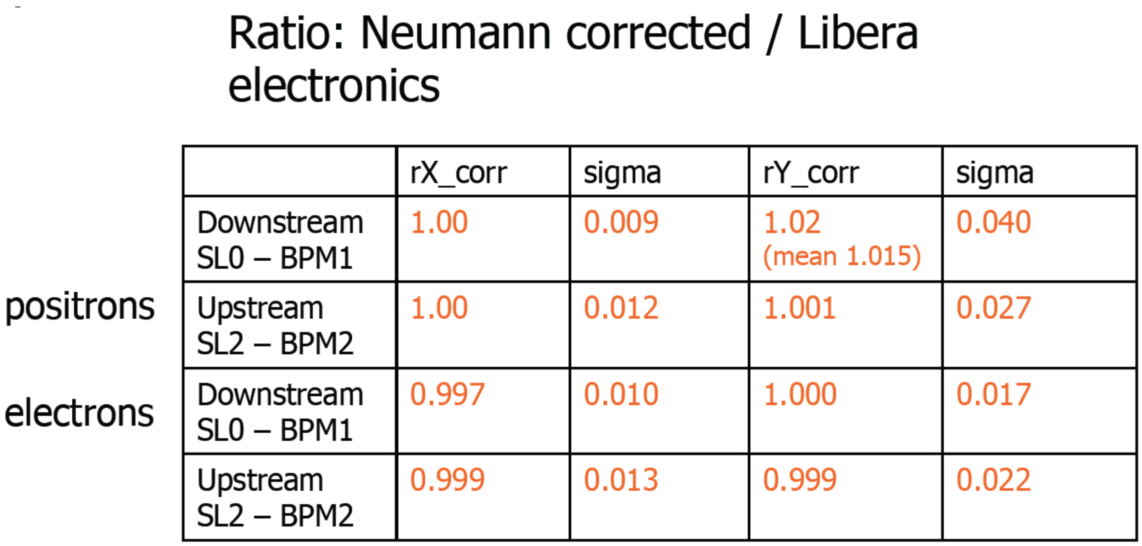

Ratio: Neumann corrected / Libera electronics

		rX_corr	sigma	rY_corr	sigma
positrons	Downstream SL0 – BPM1	1.00	0.009	1.02 (mean 1.015)	0.040
	Upstream SL2 – BPM2	1.00	0.012	1.001	0.027
electrons	Downstream SL0 – BPM1	0.997	0.010	1.000	0.017
	Upstream SL2 – BPM2	0.999	0.013	0.999	0.022

Figure 5

3.3 12° GEM and MWPC Detectors

- On closer inspection of the GEM efficiency, B. Henderson (MIT) and Ö. Ates (Hampton), it was discovered that several APV problems existed resulting in a noticeable pattern of inefficiency which was averaged over by the clustering algorithms and large bin size used previously (see **??**.
- The resulting GEM efficiency varies from 90–93 %. Some improvement can be made by averaging neighboring channels and new clustering algorithms but this must be now incorporated into the MC simulation for the GEMs. Ultimate GEM efficiency will likely be around 94 %.
- Fortunately, the MWPC efficiency remains very high. With a few dead wires visible in **??** the MWPC overall efficiency is 97–99 % and even the area near the dead wires can be recovered by requiring just two of the three XUV planes. Work by D. Veretennikov (PNPI) and B. Henderson (MIT).
- Even with the reduced efficiency of the GEM detectors tracking through the 12° telescopes should still be very efficient by allowing 4, 5, or 6-fold coincidences.

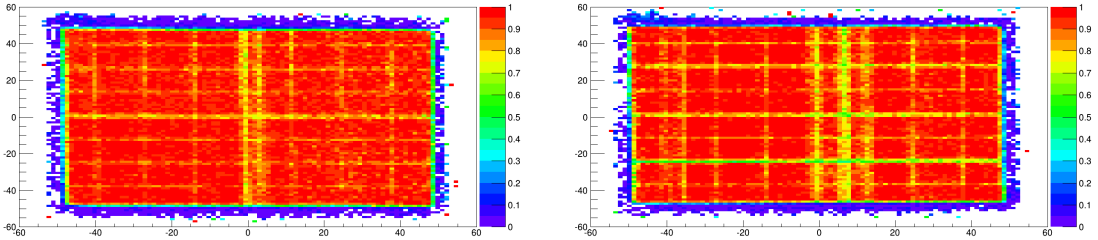

(a) Downstream Left (b) Downstream Right

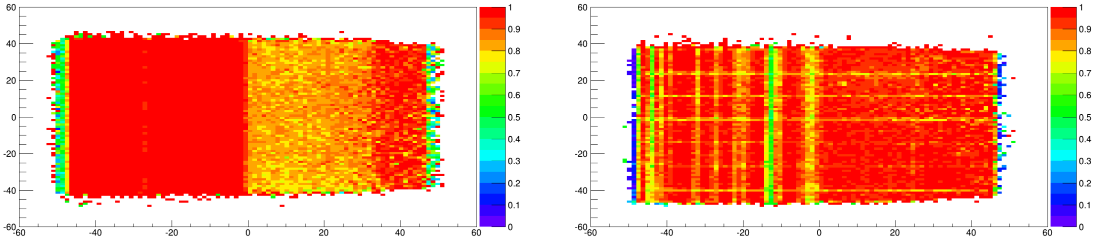

(c) Middle Left (d) Middle Right

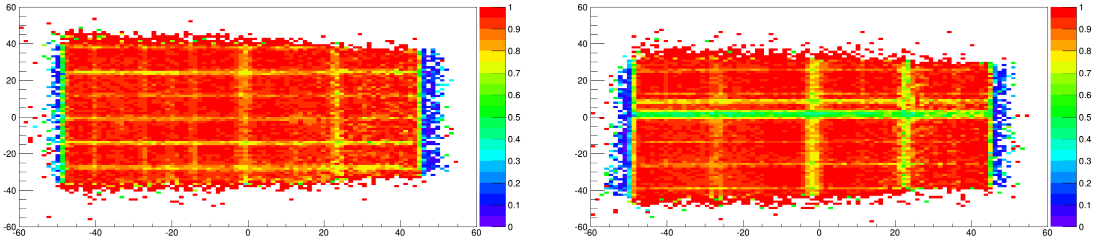

(e) Upstream Left (f) Upstream Right

Figure 6: GEM detector efficiencies.

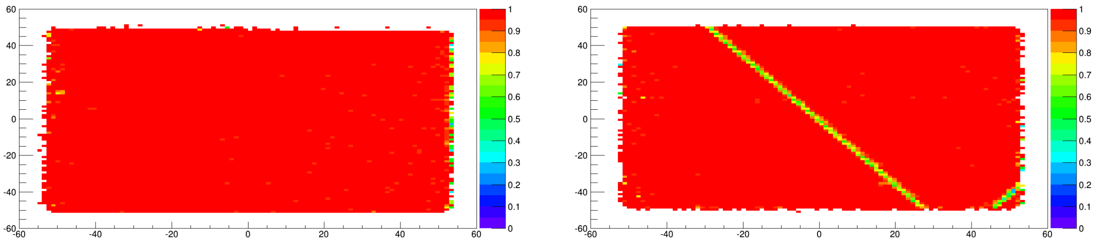

(a) Downstream Left (b) Downstream Right

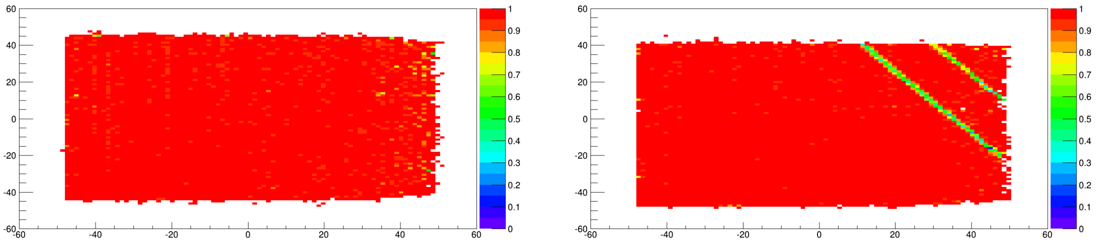

(c) Middle Left (d) Middle Right

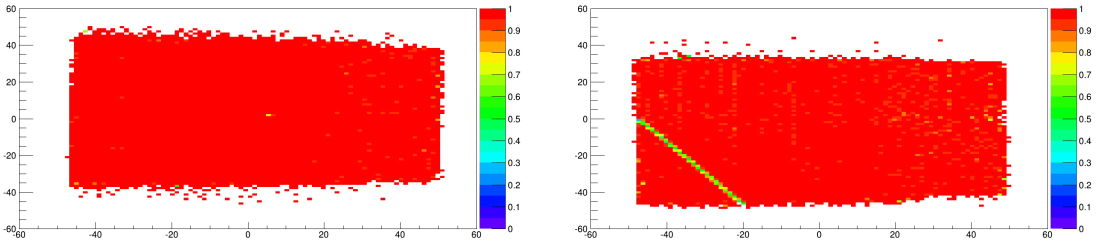

(e) Upstream Left (f) Upstream Right

Figure 7: MWPC detector efficiencies.

3.4 Time of Flight Detectors

- With tracking extrapolated (see below) to the TOF detectors it is possible to continue and improve the calibration.
- L.D. Ice (ASU) and others have analyzed the extrapolated track. Fig. 8 shows the difference between the TOF bar number predicted by the tracking and that actually hit.
- Similarly there is a strong correlation between the vertical position from tracking and that reconstructed from the time difference between the top and bottom PMTs (see Fig. 9).
- The resolution around 100 mm is consistent with that achieved at BLAST.
- Fig. 10, L.D. Ice (ASU), shows the momentum versus time of flight for leptons and protons. At higher momenta the separation is not so clear. J. Bernauer (MIT) is investigating improving this by correcting the time of flight by the actual path length.
- Electrons and protons are of course separated by their charge and opposite curvatures in the magnetic field. But distinguishing positrons and protons will require a probabilistic approached based on these momentum versus time figures.
- R. Russell (MIT) has investigated the energy deposited in the TOF as a function of the time of flight. The expected “sail” figure for protons is clear in Fig. 11. This can then be used to calibrate and monitor the gain. The same effect is nicely reproduced in the Monte Carlo (same figure) lending confidence to the TOR simulation.

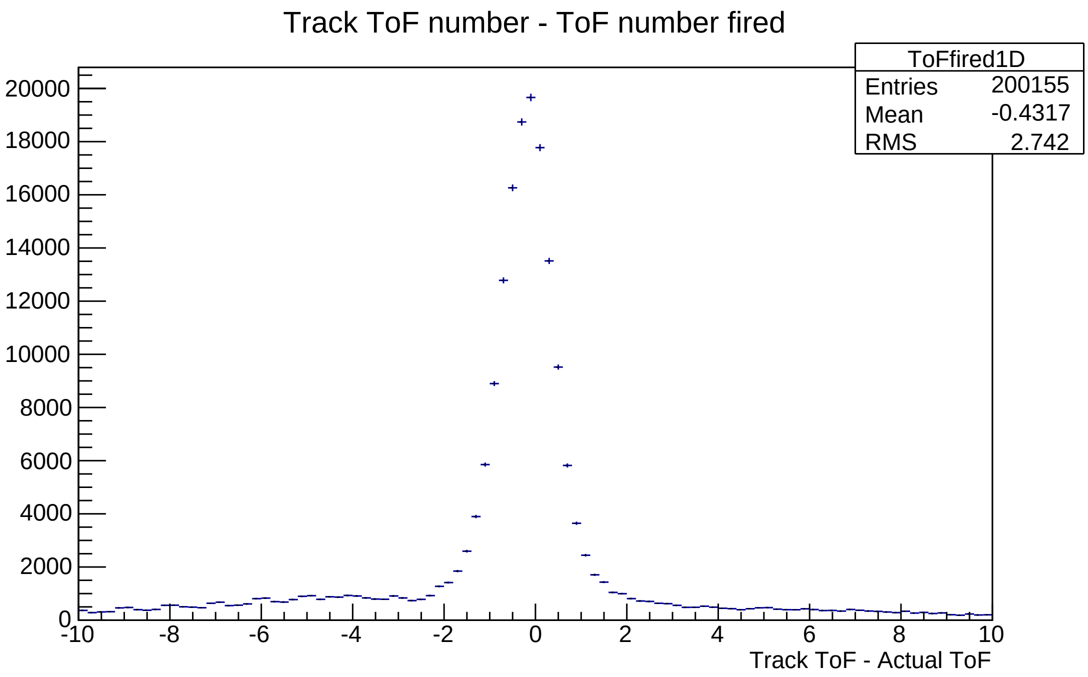

Figure 8: Difference between TOF bar number extrapolated from tracking and as found in data.

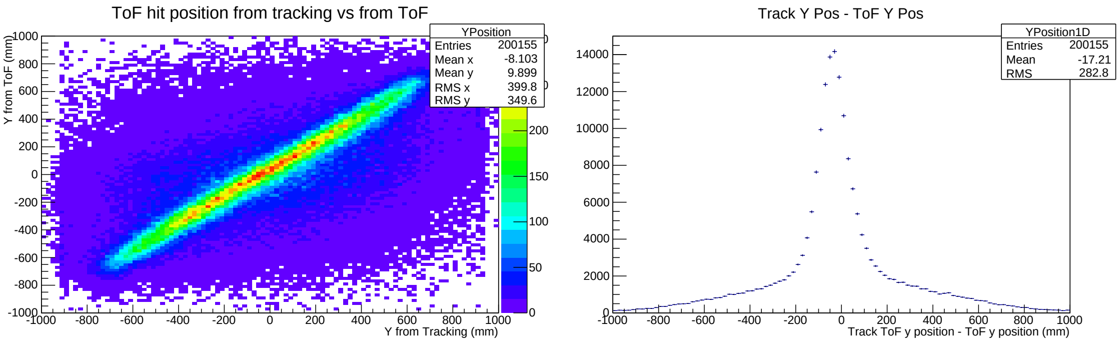

(a) 2D

(b) Projection

Figure 9: Comparison of vertical position in TOF from data and extrapolated from tracking.

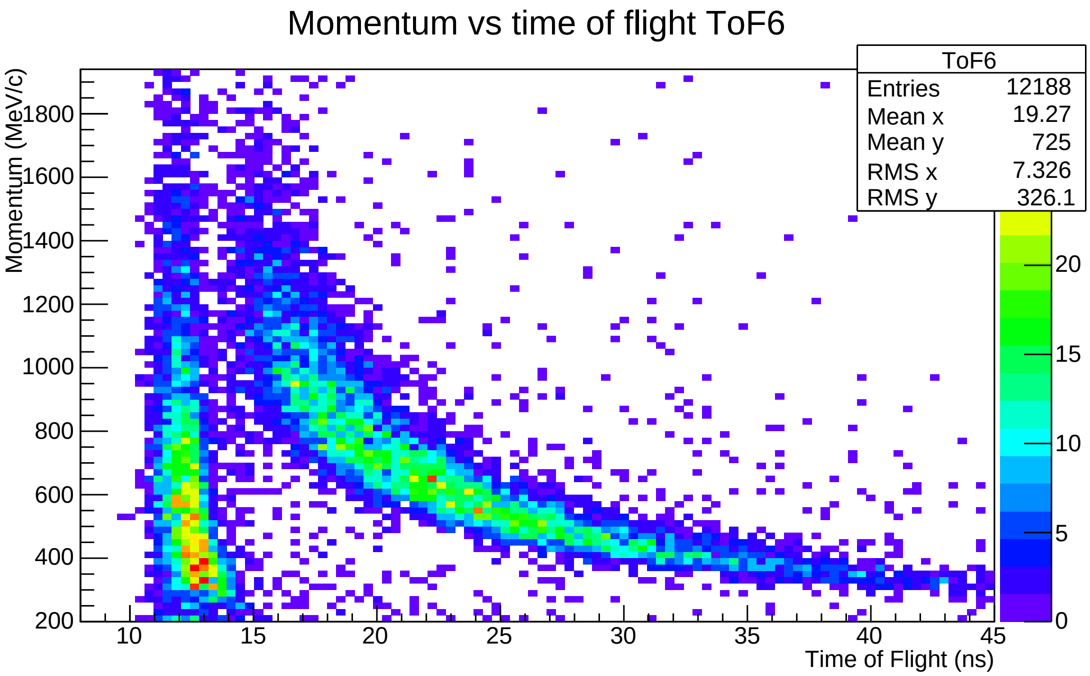

Figure 10: Momentum versus time of flight for ToF bar 6.

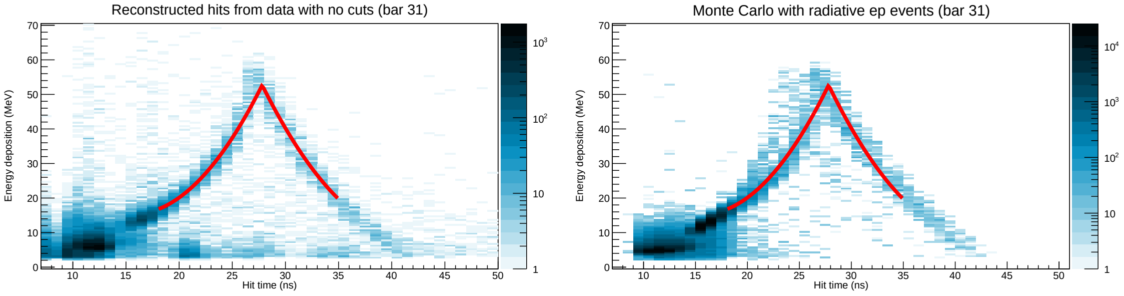

(a) Data

(b) Monte Carlo

Figure 11: Energy deposited in TOF bar 31 as a function of the hit time from data and in Monte Carlo simulation.

4 Track Reconstruction

- The main track reconstruction remains the elastic arm algorithm implemented by J. Bernauer (MIT). This fits the time to distance relationship by analyzing a large collection of tracks accounting for multiple scattering and energy loss.
- The yield as shown previously is given in Fig. 12.
- The coplanarity, $< \pm 2^\circ$, after cuts on the momentum balance and vertex is shown in Fig. 13.
- The momentum resolution, $\Delta P/P = 0.12$, is shown in Fig. 14.
- As previously mentions the tracking has been extrapolated to the time of flight detector (see above).
- The tracked data has also been released to the collaboration so that everyone can start developing their own analyses. Some of these will be shown in the next section.

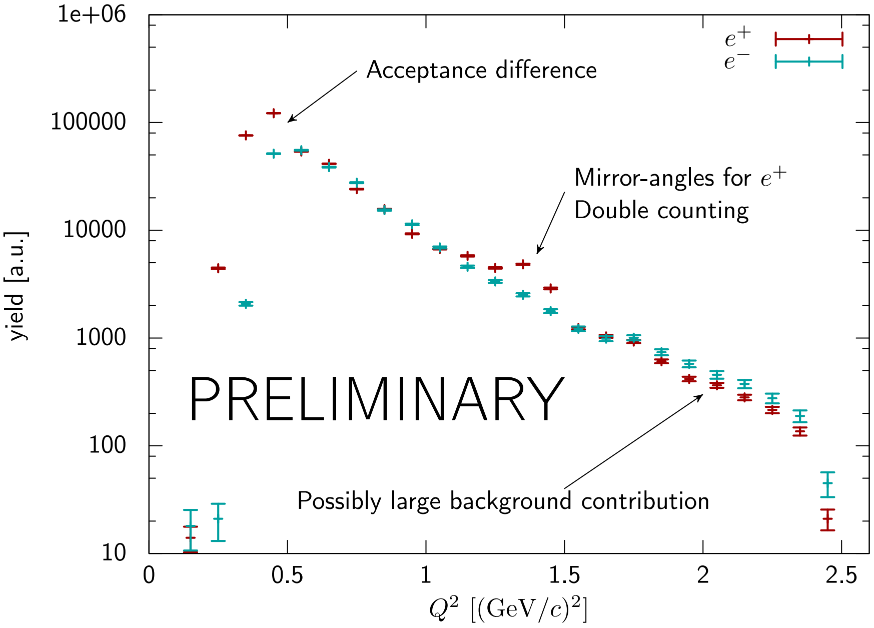

Figure 12: Yield for elastic e^-p and e^+p scattering as a function of Q^2.

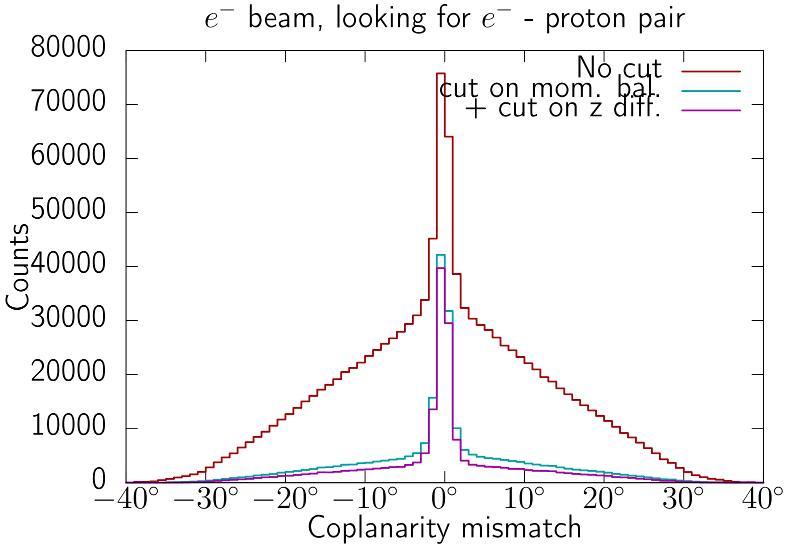

Figure 13: Track coplanarity before and after cuts on the momentum balance and vertex.

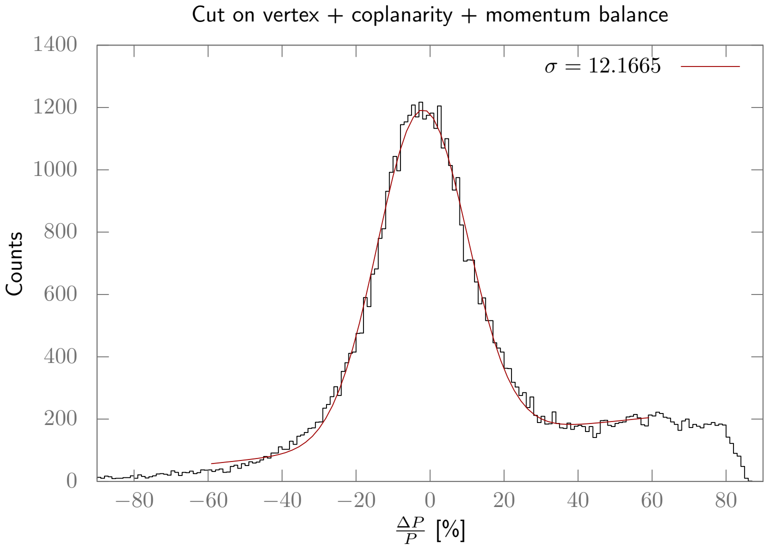

Figure 14: Track momentum resolution.

4.1 Alternative, Traditional Track Reconstruction

- Track reconstruction in the OLYMPUS wire chambers is not trivial. The inhomogeneous magnetic field means every drift cell has a different time to distance relationship. Furthermore this relationship varies to the left and right of each sense wire and each sense wire in a cell is different.
- Using MagBoltz it is possible to calculate gas properties. These can then be used in a field mapping program like Garfield to determine lines of electron drift and isochrones (see **??**).
- The tangent point to each isochrone, extrapolated to the point where it crosses the sense wire plane gives the distance from the sense wire for that track angle, drift time, sense wire, magnetic field, and side (left or right) of the sense wire.
- The range of distance versus time is large (see **??**).
- For a well defined condition: fixed track angle, fixed field, fixed sense wire, fixed side of the sense wire the time to distance relationship is fairly simple (see Fig. 17). A cubic polynomial near the wire with a linear polynomial in the main drift region.
- D. Hasell (MIT) has derived a fairly simple parameterization which gives the coefficients for the polynomials as a function of the field, track angle, wire number, and side. The residual between this parameterization and the data from the field map is shown in Fig. 18. The deviation is mostly $< \pm 0.5$ mm which is comparable to the 1 mm stagger in the sense wires in a cell. However, this is based on assuming we know the gas mixture, that MagBoltz correctly calculates the gas properties, and that the field mapping program correctly models the drift cells.
- It is likely that this approach will just provide a starting point for track reconstruction and that the parameterization will have to be optimized by iterating over the found tracks.
- Nevertheless this work has begun and the preliminary result for finding track "stubs" in a super-layer of the wire chamber is shown in Fig. 19. The main peak indicates a resolution around 400 μm which is consistent with what was obtained at BLAST. However, there are also mis-identified "stubs" and a sizable background.
- Work will continue to improve this and to connect the "stubs" to form tracks.

- Even if this work doesn't end as a reasonable production track reconstruction it can help understand the track reconstruction process possibly supplying track candidates for the elastic arm algorithm. The parameterization could also be applied inside the elastic arm algorithm.
- The parameterization can also be used in digitizing the wire chamber hits in the Monte Carlo.

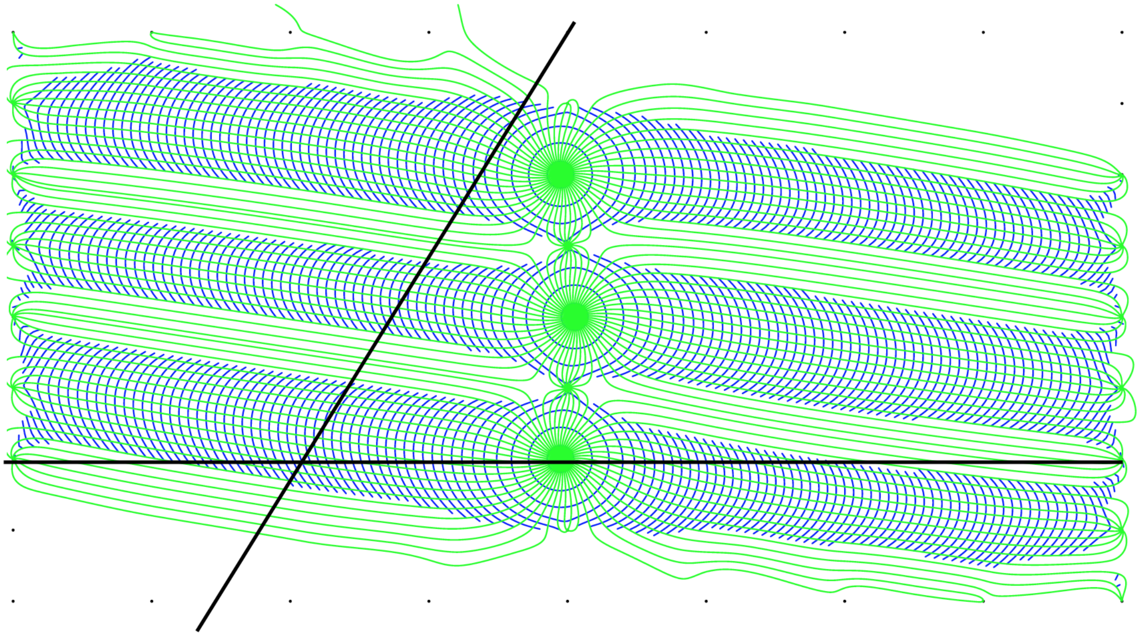

Figure 15: Fieldmap for a single drift cell showing lines of electron drift (green) and isochrones (blue). The desired reconstructed position for a track (angled line) is the point where the track crosses the sense wire plane (horizontal line).

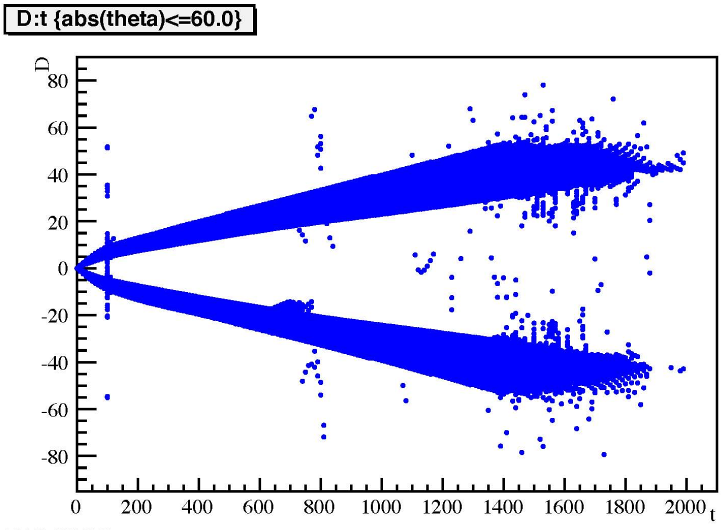

2014-01-16 10:54:34

Figure 16: Drift distance versus drift time for all sense wires in a cell, all possible magnetic fields, the possible range of track angles, and for left (positive) and right (negative) sides of the wire.

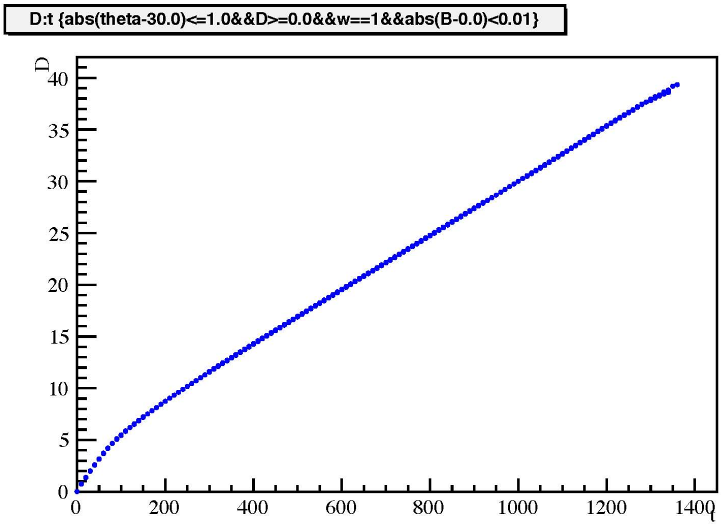

2014-01-16 12:09:59

Figure 17: Distance versus drift time for a well defined condition.

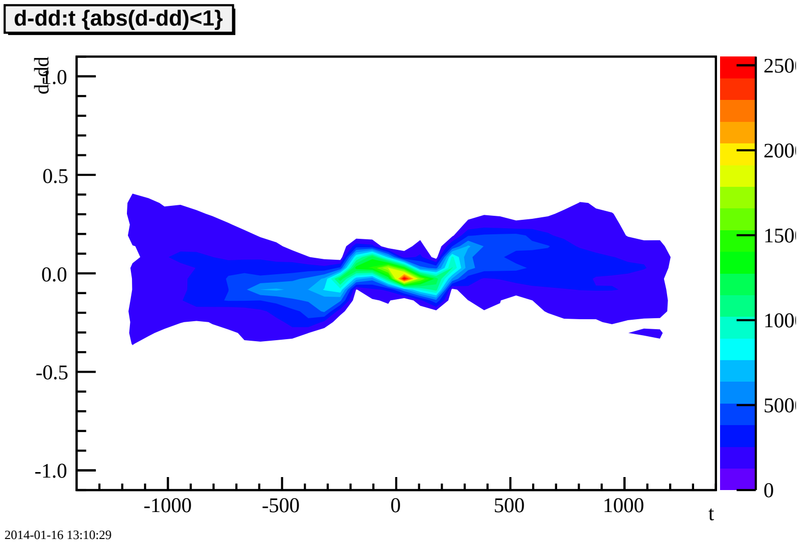

Figure 18: Difference between parameterization of time to distance relation and the input data genetated by the field map program and gas properties.

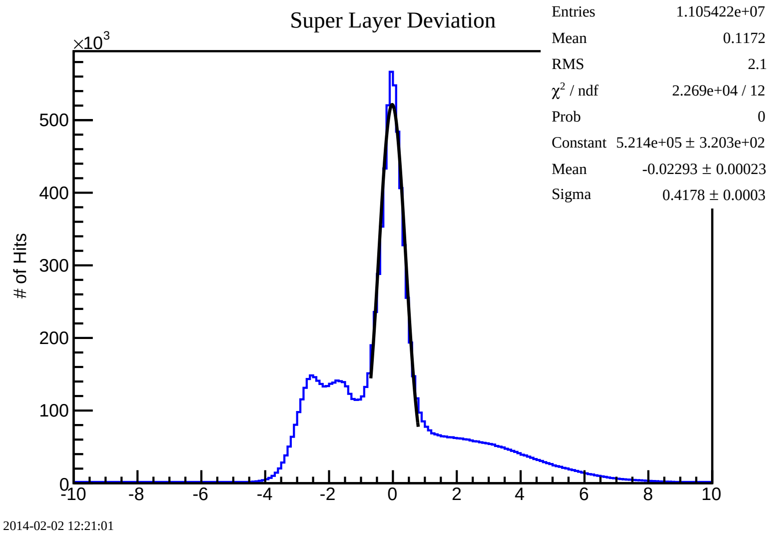

Figure 19: Residual from fitting a straight line to a track "stub" in a super-layer of the OLYMPUS wire chambers.

5 Analysis

The following analyses were performed by N. D'Ascenzo (DESY) and N. Akopov (AANL) using the tracked data sets provided from the elastic arm algorithm as previously described.

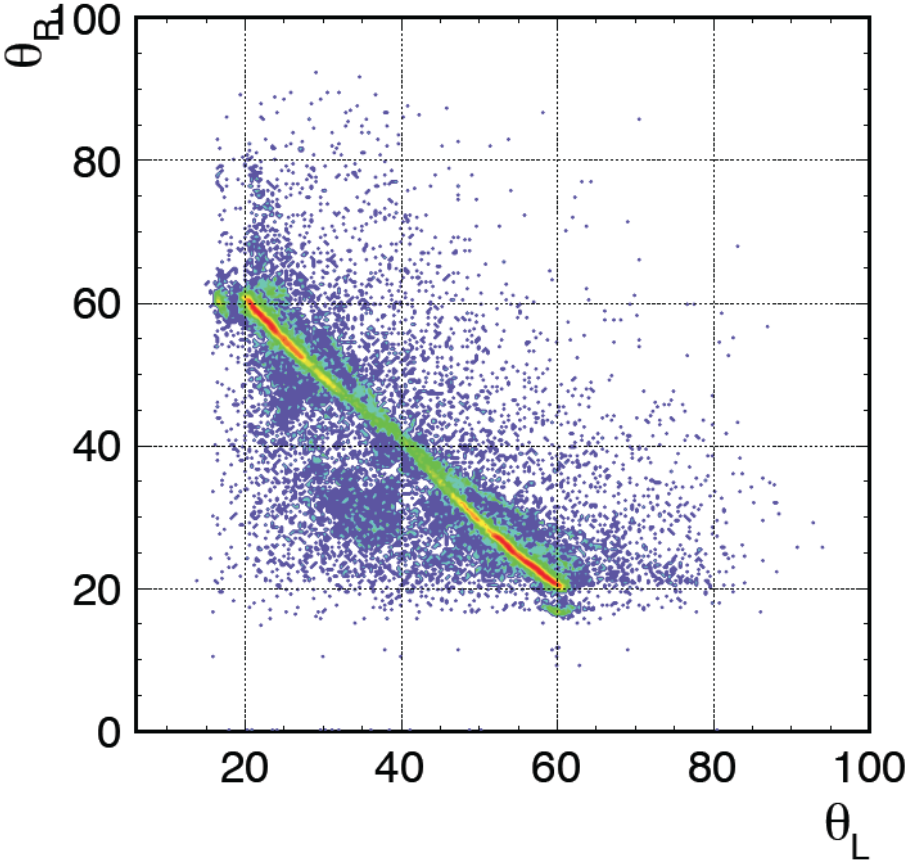

Figure 20: Angular correlation between scattering angle measured in the left sector versus the angle in the right sector. Event selection required reconstructed beam energy to be within 200 MeV and tracks to be coplanar within 4°. - N. D'Ascenzo (DESY)

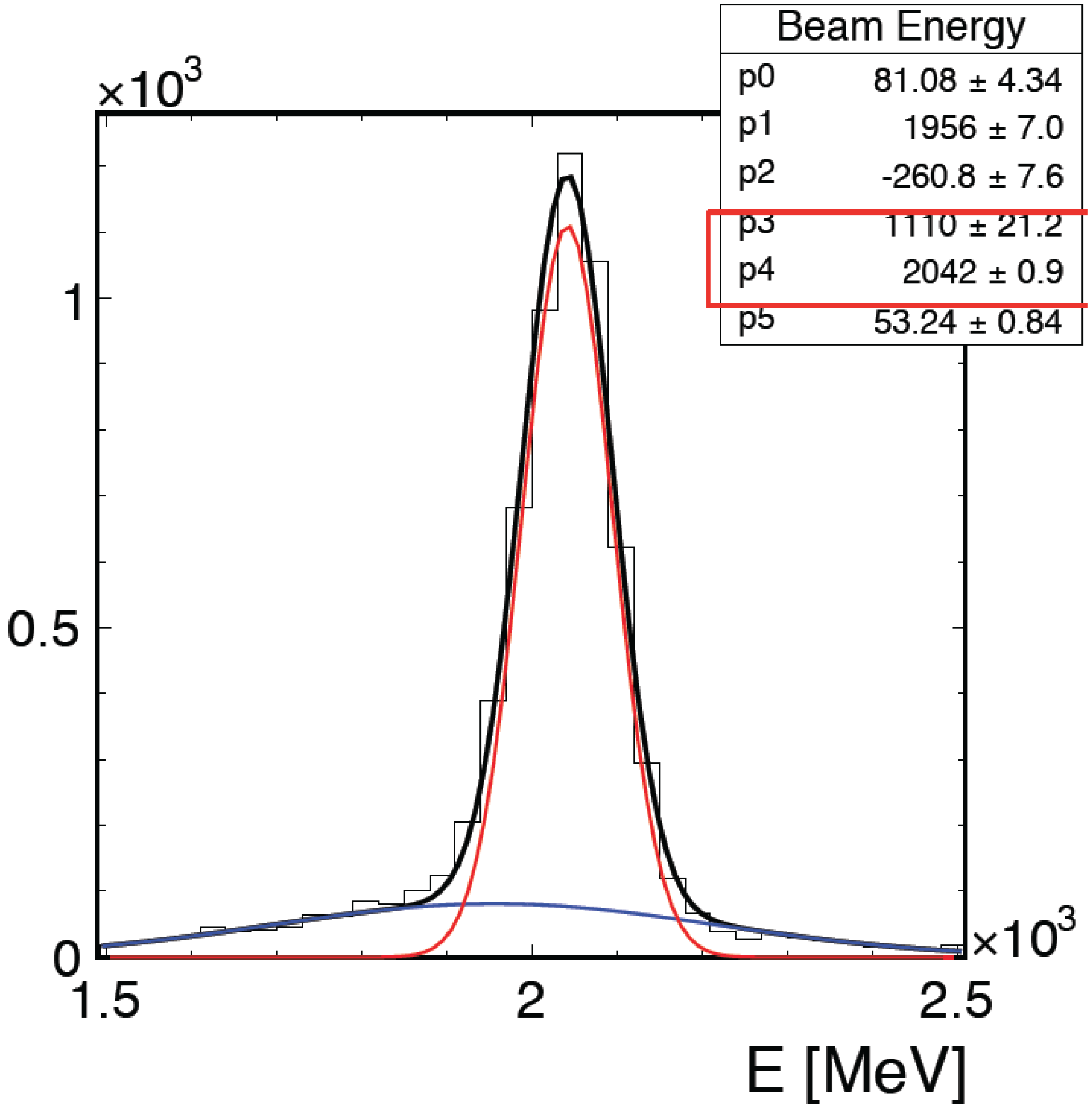

Figure 21: Beam energy reconstructed from lepton and proton scattering angles for lepton scattering angles in the range 32°–40°. - N. D'Ascenzo (DESY)

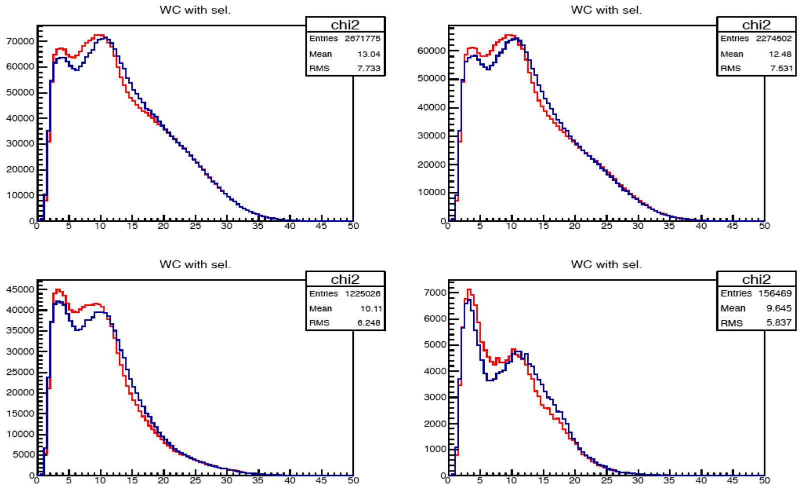

Figure 22: χ^2 distribution for electrons tracks in the left (blue) and right (red) sectors for progressive cuts on the event selection. - N. Akopov (AANL)

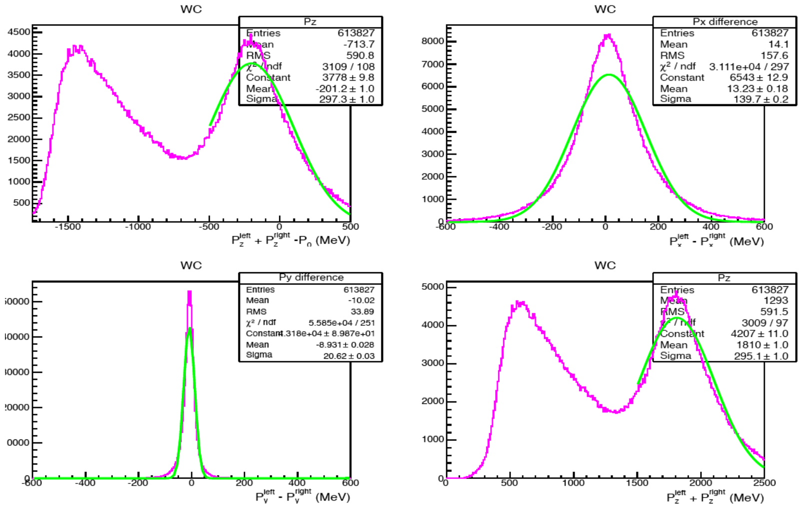

Figure 23: Reconstructed beam energy and reconstructed x, and Y components of momentum. - N. Akopov (AANL)

5.1 Radiative Corrections

- R. Russell (MIT) and A. Schmidt (MIT) have taken the Mainz generator (J. Bernauer) and incorporated into the OLYMPUS Monte Carlo framework incorporating radiative corrections.
- The radiative corrections include:soft two photon exchange, vertex corrections including self-energy, initial and final state bremsstrahlung for both lepton and proton, and vacuum polarization. It does not include hard two photon effects.
- The radiative corrections agree with Maximon and Tjon in the low energy limit.
- The radiative corrections are intended to be part of a common code package for use by all the two-photon experiments (Jlab and Novosibirsk) to simplify comparing results.
- The MIT code has been tested and compared with the Novosibirsk code and found to agree as illustrated to the following plots Fig. 24 which shows and compares the invariant matrix element as a function of the lepton polar angle and lepton momentum for photon scattering angles $\theta = 10^\circ$ and $\phi = 120^\circ$ and lepton azimuthal angle $\phi = 0^\circ$

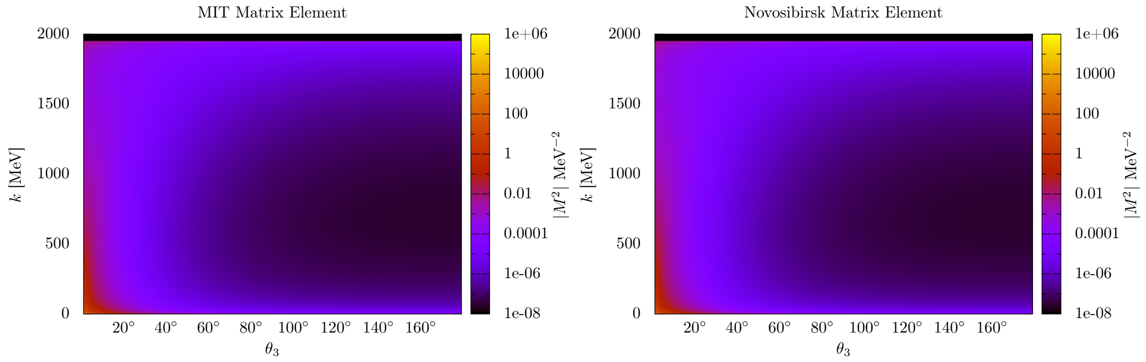

(a) M.I.T.

(b) Novosibirsk

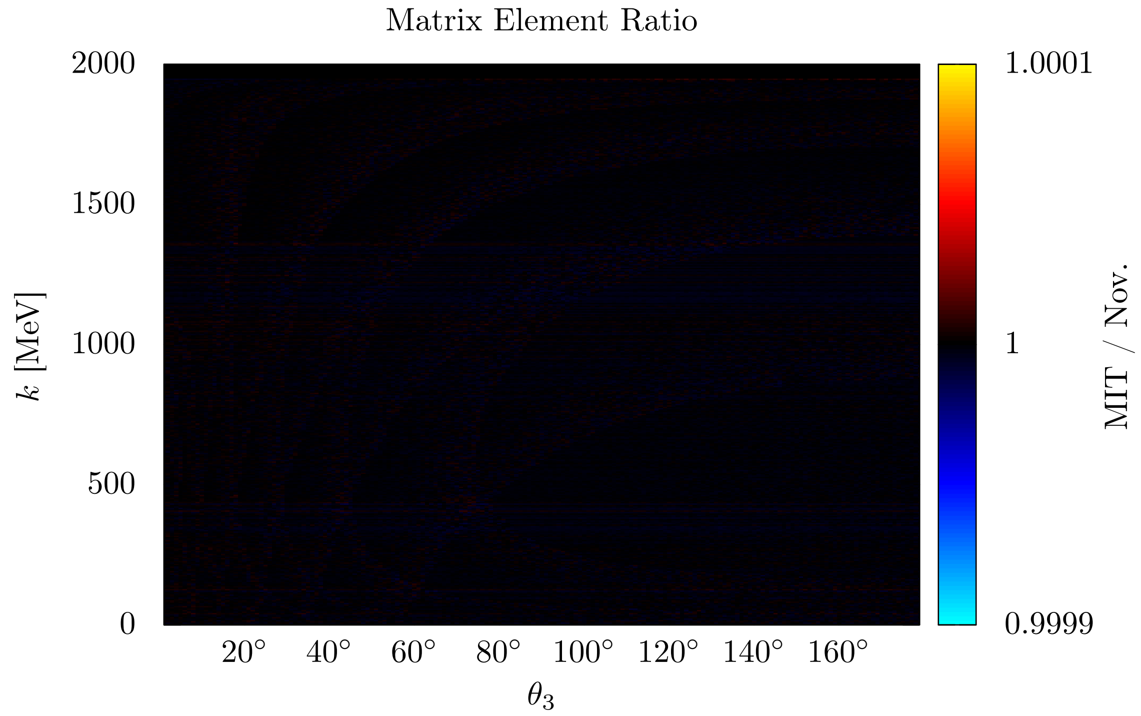

(c) Difference

Figure 24: Comparison of radiative corrections calculated using the MIT and Novosibirsk generators.

6 Miscellaneous

- The NIMA paper describing the experimental hardware, electronics, and operation accepted for publication - R. Milner, et al. The OLYMPUS Experiment, NIMA (2013), 10.1016/j.nima.2013.12.035.
- A paper describing the OLYMPUS target and vacuum system is nearly ready for submission to NIM.
- A. Schmidt (radiative corrections) will give a talk at APS, Savannah, March 3–7, 2014.
- The next OLYMPUS collaboration meeting will be held at Mainz, March 10–12, 2014 and include a day workshop specifically to address issues with the luminosity monitors.
- J. Diefenbach with give a talk on OLYMPUS at the DPG meeting in Frankfurt, March 17–21, 2014.
- R. Perez Benito (SYMB) and R. Russell (radiative corrections) with also give talks at DPG.
-

7 Summary

The analysis of the OLYMPUS data collected in 2012 is difficult and complex but steady progress is being made. More people are active in the analysis. The results obtained to date are encouraging and hopefully indicate that a good, final results will eventually be obtained.